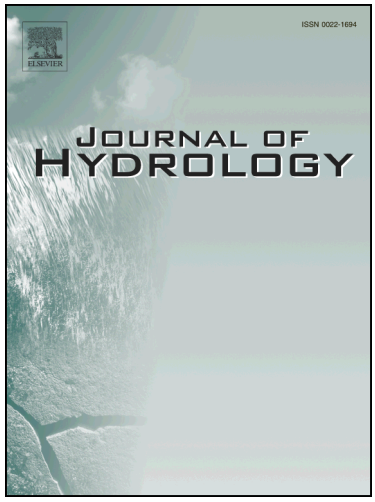

Research papers

On the estimation of spatially representative plot scale saturated hydraulic conductivity in an agricultural setting

Tommaso Picciafuoco, Renato Morbidelli, Alessia Flammini, Carla Saltalippi, Corrado Corradini, Peter Strauss, Günter Blöschl

PII: S0022-1694(19)30019-8
DOI: https://doi.org/10.1016/j.jhydrol.2018.12.044
Reference: HYDROL 23371

To appear in: *Journal of Hydrology*

Received Date: 18 September 2018
Revised Date: 10 December 2018
Accepted Date: 12 December 2018

Please cite this article as: Picciafuoco, T., Morbidelli, R., Flammini, A., Saltalippi, C., Corradini, C., Strauss, P., Blöschl, G., On the estimation of spatially representative plot scale saturated hydraulic conductivity in an agricultural setting, *Journal of Hydrology* (2019), doi: https://doi.org/10.1016/j.jhydrol.2018.12.044

On the estimation of spatially representative plot scale saturated hydraulic conductivity in an agricultural setting

Tommaso Picciafuoco[a,b,*], Renato Morbidelli[a], Alessia Flammini[a], Carla Saltalippi[a], Corrado Corradini[a], Peter Strauss[d], Günter Blöschl[b,c]

[a] Dept. of Civil and Environmental Engineering, University of Perugia, via G. Duranti 93, Perugia, Italy

[b] TU Wien, Centre for Water Resource Systems, Karlsplatz 13, A-1040, Vienna, Austria

[c] TU Wien, Institute of Hydraulic Engineering and Water Resources Management, Karlsplatz 13, A-1040 Vienna, Austria

[d] Federal Agency for Water Management, Institute for Land and Water Management Research, A-3252 Petzenkirchen, Austria

Abstract

Spatially representative estimates of saturated hydraulic conductivity, K_s, are needed for simulating catchment scale surface runoff and infiltration. Classical methods for measuring K_s are time-consuming so sampling campaigns need to be designed economically. Important insights can be obtained by experiments directed to understand the controls of K_s in an agricultural setting and identify the minimum number of samples required for estimating representative plot scale K_s. In this study, a total of 131 double-ring infiltrometer measurements were made on 12 plots in a small Austrian catchment. A statistical analysis of K_s across the catchment suggests K_s to be only slightly influenced by physical and topographical soil characteristics while land use is the main control. The highest values of K_s were observed in arable fields, with a median of about 3 times and a coefficient of variation (CV) of about 75% of those in grassland areas. An uncertainty analysis aimed at determining the minimum number of K_s measurements necessary for estimating the geometric mean of K_s over a given area with a specified accuracy suggests that, beyond a specific and plot-size dependent number of measurements, the benefit of any extra measurement is small. The confidence interval of the geometric mean of K_s decreases with the number of measurements and increases with the size of the plot sampled. Applications of these findings for designing field campaigns are discussed.

Keywords: saturated hydraulic conductivity, local measurements, spatial variability, plot-scale estimate

* Corresponding author
e-mail address: tommaso.picciafuoco@unifi.it (T.Picciafuoco)

1 Introduction

The hydraulic conductivity of saturated soils, K_s, is a key parameter controlling various hydrological processes, including rainfall partitioning into infiltration and surface runoff. Accurate estimates of K_s are needed for modeling local infiltration into homogeneous (Parlange et al., 1982) and layered soils (Govindaraju et al., 2012), as well as for upscaling infiltration models (Smith and Goodrich, 2000; Corradini et al., 2011). Saturated hydraulic conductivity is highly variable in space due to soil structure (Dexter et al., 2004), texture (Saxton et al., 1986; Jabro, 1992), landscape position (Mohanty et al., 1994), and land cover and management practices (Alletto and Coquet, 2009; Bonell et al., 2010), it also depends on scale (Sobieraj et al., 2004; Lai and Ren, 2007). Saturated hydraulic conductivity typically varies even more than two orders of magnitude in space. Baiamonte et al. (2017) performed 150 infiltration measurements in a Sicilian basin and observed values of K_s that ranged from less than 1 mm h^{-1} to more than 8000 mm h^{-1}. Papanicolaou et al. (2015) conducted about 120 infiltration experiments on three hillslopes with different agricultural management practices in Iowa and observed K_s values that ranged from 0.15 mm h^{-1} to 360 mm h^{-1}. Similarly, Loague and Gander (1990) carried out 157 infiltration measurements in a small rangeland catchment of area 0.1 Km^2 (R-5, Oklahoma) and obtained values of K_s approximately variable by two orders of magnitude in space. Furthermore, Sharma et al. (1987) performed infiltration experiments in two lateritic Australian catchments (0.94 Km^2 and 0.81 Km^2) and found K_s values in the range 8.33-946 mm h^{-1} and 237-1646 mm h^{-1}, respectively.

Woolhiser et al. (1996) found that runoff hydrographs were strongly affected by variations in saturated hydraulic conductivity at the hillslope scale, especially for small runoff events. Taskinen et al. (2008) investigated the effects of spatial variability of K_s on overland flow in a small agricultural catchment by analyzing 2000 synthetic rainfall-runoff events generated from observed rainfall events with runoff modelled using different spatially variable K_s fields. They found the greatest differences in the first flow peak and in the rising part of the hydrograph. Hu et al. (2015) analyzed the effects of K_s variability on runoff simulations in a small watershed on the Chinese Loess Plateau and found that total and peak discharges were underestimated if the spatial variability of K_s was completely ignored or only partially considered. Assouline and Mualem (2002) examined the effects of the spatial variability of soil hydraulic properties combined with

the formation of a sealing layer at the soil surface. They deduced that the hydrological response of arid and semiarid catchments is dominated by these effects. Assouline and Mualem (2006) showed that infiltration into crusted soils experiences substantial changes for the presence of K_s spatial heterogeneity , particularly for loam soils. Accounting for K_s spatial variability is therefore essential.

In addition to undisturbed soil core sampling, several experimental techniques are available for estimating K_s through in-situ infiltration measurements. The most commonly used devices are: tension permeameters, e.g. the CSIRO disc permeameter (Perroux and White, 1988), single ring infiltrometers (Lassabatère et al., 2006; Bagarello et al., 2004, 2014a; Ahmed et al., 2014), double-ring infiltrometers (Swartzendruber and Olson, 1961), constant-head well permeameters, e.g. the Guelph permeameter (Reynolds and Elrick, 1985), and rainfall simulators, e.g. the Guelph rainfall simulator (Tossell et al., 1987). The device choice conditions the estimated values of K_s (Verbist et al., 2013; Bagarello et al., 2014a) due to different factors (Reynolds et al., 2000) such as size of investigated soil, sample collection procedure, flow geometry, and estimate of other soil parameters (e.g., soil sorptivity, saturated water content) necessary to derive the value of K_s applying specific data analysis procedures.

Widely used techniques to determine K_s, such as the traditional well permeameter and ring infiltrometer, rely on the attainment of a steady-state flow rate, so that the time required to carry out each measurement is usually high. Other techniques do not require to achieve steady conditions (Bagarello et al., 2004; 2014b) but, in any case, their use at the catchment scale represents a challenge. Speeding up the measurement operations with the purpose of achieving detailed K_s maps over large areas is therefore one of the greatest issues to be addressed in spatial infiltration studies. Pedotransfer functions which estimate K_s from more easily measurable soil physical properties (Bouma, 1989) and statistical approaches to extrapolate K_s from a small number of measurements to the entire catchment are some of the approaches adopted to reduce the time demand of extensive field measurement campaigns.

However, macropores and other preferential flow paths often dominate the infiltration behavior even more than the characteristics of the soil matrix (as quantified by porosity, texture etc.), so it is usually advantageous not to rely only on pedotransfer functions from the literature but to perform at least a few K_s measurements in the catchment of interest (Bouma et al., 2011). Regarding the number of measurements required, Vieira et al. (1981) studied the spatial variability of 1280 field-measured infiltration rates using

geostatistical concepts. They argued that 128 samples were sufficient to obtain nearly the same information as obtained from 1280 samples. Ahmed et al. (2015) conducted an uncertainty analysis on 722 infiltration measurements in six roadside drainage ditches (grassy swales, i.e. shallow, open vegetated roadside drainage channels designed to convey stormwater runoff to storm sewers or water receiving bodies) and concluded that approximately twenty infiltration measurements were the minimum number to obtain a representative geometric mean of K_s of a swale that was less than 350 m long, with an acceptable level of uncertainty. The identified minimum number was related to the width of the 95% confidence interval that in logscale was about equal to 2.

Skøien and Blöschl (2006) found that the required number of samples depends on the spatial correlation of K_s as well as on the measurement setup. They investigated the effect of spacing (average distance between samples), extent (size of the domain sampled) and support (averaging area of one sample), i.e. the "scale triplet" as termed by Blöschl and Sivapalan (1995), on the estimates of mean, spatial variance and complete range of a variable in a landscape. For each of the chosen combinations of spacing, support and extent they generated 1000 synthetic random fields and sampled from them according to the selected scale triplet. In what they termed "single realization case", they compared the sample mean and sample variance with the mean and variance of the entire random field of the same realization. They found that the estimation uncertainty of the mean increases when the spacing increases for a given number of samples. Small extents (relative to the underlying correlation length) imply that the samples are highly correlated and the underlying distribution can be well characterized from a limited number of samples. Skøien and Blöschl (2006) used numerically generated random fields, and actual observations of K_s may differ in terms of their sampling characteristics. Also, by identifying the controls on K_s, areal estimates can be improved over random sampling, either by stratified sampling or by making use of pedotransfer functions.

The main objective of this paper is to identify the main elements that control the soil saturated hydraulic conductivity in an agricultural setting and, on this basis, to define the minimum number of samples needed for estimating a value of K_s representative at the plot scale. This is a crucial element to obtain the first of the two moments of the K_s probability density function required to apply areal infiltration modeling (Flammini et al., 2018). The results of K_s measurement campaigns performed in a small catchment in Austria with double-ring infiltrometers (DRIs) are used. The choice of this equipment was made on the basis of a few

practical considerations later specified and mainly of the outcomes earlier obtained by Morbidelli et al. (2017) in laboratory experiments finalized to compare a double-ring infiltrometer, a tension permeameter and a constant-head well permeameter using controlled rainfall-runoff experiments as a benchmark. Measurements collected in both grasslands and arable lands are selected to deduce the effects of different land management operations on the K_s spatial variability. A statistical analysis is performed to understand the confidence in the estimate of the areal average value of K_s for different land uses, plot areas and sample sizes. Based on this analysis, guidance is given for planning measurement campaigns with double-ring infiltrometers when time and resources are limited.

2 Materials

2.1 Study area

The study area is the Hydrological Open Air Laboratory (HOAL) catchment located in Petzenkirchen, in the western part of Lower Austria. The basin has an area of 0.66 km^2. The elevation ranges from 268 to 323 m a.s.l. with a mean slope of 8%. Landcover consists of arable land (87%), pasture (5%), forested area with grassland and high-stemmed vegetation of low density (6%), and paved surfaces (2%) (Blöschl et al., 2016). In this study, pasture and forested area are collectively denoted as “grassland areas” because the forested area is really characterized by grassland, and not by brushwood, as a result of the patchy type of land use that takes place in the catchment. The climate is humid with a mean annual temperature of 9.5°C and a mean annual precipitation of 823 mm yr^{-1} from 1990 to 2014.

A soil survey campaign of 300 cores, sampled on a 50×50 m grid, provided information about organic matter content (*om*), clay (*cl*), silt (*si*), and sand (*sa*) percentages at multiple depths. According to the USDA soil classification, the topsoil in the catchment consists of silt loam (75% of the area), silty clay loam (20%), and silt (5%). A high-resolution digital terrain model (DTM) was used to derive elevation (*el*) and local slope angles (*s*) across the catchment.

Winter wheat, winter barley, maize, rapeseed and soy are the main types of crop cultivated in the catchment. Crop rotation is associated with green manure in order to ensure natural fertilization of the soil. However, nitrogen fertilizers and natural fertilizers, e.g. pig manure, are also applied before sowing, as well as plant protection agents, such as plant growth regulators, fungicides and broad-spectrum insecticides. The

harvest of the winter crops usually occurs in July, allowing the access to the cultivated areas for infiltration measurements until the late-August/September when field preparation for tillage and seedbed is made.

2.2 Soil data collection

A total of 131 locations, on 12 different plots, were chosen to sample K_s of the soil surface of the HOAL catchment (Figure 1). The measurements were performed with the objective of evenly exploring the grassland areas, specifically those without high-stemmed vegetation, and the areas devoted to agricultural practices. Depending on the time required to perform a local experiment by the selected procedure (described below), the measurements in each plot were carried out in a narrow period, up to 3 days for the larger plot. The measurements in the whole grassland areas were substantially completed in the period March 15 – April 7, while in the cultivated areas, due to restricted access during the crop growing season and tillage operations, the experimental campaign was made in the period between harvest and tillage. In the last period, between July 20 and September 20, it was possible to investigate different plots at the same condition with respect to agricultural practices even though at different times. In any case, because of the absence of bare soils subjected to significant temporal changes of K_s due to crust formation and disruption, the lack of measurements contemporaneity should not have significantly affected the main features of the K_s spatial heterogeneity field.

Among the available measurement techniques, DRIs were considered to be appropriate because of the ease of installation and robustness in natural environments where tall grass, surface slope or strong wind may preclude the usage of other, more sensitive, devices. Due to the equipment low cost, simultaneous use up to four instruments was possible to speed up the experiments. The technique consists of pushing two concentric steel rings, of diameters 0.3 m and 0.6 m, about 10 cm into the ground and pouring water inside them until the water level equalizes in the two rings. The reduction of the inner ring water level due to infiltration is recorded at regular time steps, and the measurement ends when infiltration steady state is obtained. In our measurements the latter was considered to occur when an infiltration rate invariant in the last hour was detected. The saturated hydraulic conductivity was assumed equal to the last value of infiltration rate, typically observed with a ponded depth of water of about one centimeter. Morbidelli et al. (2017) showed that DRIs tended to overestimate the areal average value of K_s as compared to controlled rainfall-runoff experiments. They also found that, when samples were taken with DRI in a highly-controlled laboratory

system characterized by a soil with homogeneous grain size distribution and bare surface, the observed values did not significantly change over the repetitions performed in adjacent places. This finding highlights that DRIs allow reliable estimates of K_s in terms of repeatability, but they are biased compared to the benchmark value. In any case, considering the measurement repeatability, it is expected that the observed bias does not significantly affect the spatial variability analysis of K_s, even though the possible existence of a bias dependent on the correct K_s values cannot be ruled out. On the other hand, the magnitude of the bias is still an open issue for any available device because of the difficulties related to the identification of an indisputable "true" reference value of K_s.

On each plot, K_s measurements were performed with a spatial resolution of 3 m. The duration of each run was typically of 3-4 h. Figure 2 highlights examples of the different environmental conditions present on the plots: Figure 2a, shows the largest plot, plot 2, which consists of grassy land and is located close to the forested area with grassland. Figure 2b represents plot 5 showing the winter wheat stubbles that remains in the field after the harvest, and Figure 2c, shows plots 11 and 12, both located in a naturally-vegetated orchard. In the choice of the measurement locations, slope represented a crucial factor. According to Philip (1991), in the initial stage of the infiltration process – when the capillary forces play a leading role – the infiltration rate does not depend on the surface inclination, but after a long time – when only gravitational forces drive the process – the infiltration rate is reduced by the cosine of the slope angle. However, experimental evidence does not always support this theoretical formulation (Essig et al., 2009; Morbidelli et al., 2015). In any case, it is widely recognized that slope affects the infiltration process. In this light to reduce the slope effects (Morbidelli et al., 2016), measurements were only performed at locations with surface slope angles generally less than 10° and in the absence of bare soils.

At the locations where the infiltration measurements were performed, soil textural composition and organic matter content were inferred from the survey data available on the 50×50 m grid. In addition, slope and elevation across the catchment were obtained from the DTM. The physical and topographical soil characteristics, displayed in Table 1, show little spatial variation between the measurement locations. The maximum Coefficient of Variation (CV) observed for textural composition and organic matter content is about 15%, consistent with the USDA soil classification of the catchment according to which only two main

soil types are identified in the basin (95% of the topsoil is either silt loam or silty clay loam). Only the surface slope angle exhibits a significant variation, with a CV of about 30%.

3 Method

3.1 Statistical analysis and controls on saturated hydraulic conductivity

The ANOVA method (Armstrong et al., 2000) has been selected for the analysis of variance of the experimental data associated to the different plots to understand whether the variability of K_s across the catchment is linked to specific soil physical characteristics of the measurement locations. An application of this method requires that specific assumptions on the experimental data are satisfied. In general terms, the results obtained for the study variable are subdivided into J groups and the ith observed value (i=1…I) of a given group, j ($j = 1, \dots, J$), can be expressed as a sum of the mean of all the available measurements, μ, the group effect, τ_j, representing the deviation of the group mean μ_j from μ and a random element, $\varepsilon_{i,j}$, reflecting the combined effects of measurement errors and natural variation through observations. The basic assumptions involved in the ANOVA method concern the random elements that should be normally distributed with the same variance in all groups, while the means μ_j can be variable from group to group. The available K_s data do not satisfy these two conditions, while log-transformed values of K_s have been found appropriate for the ANOVA method application (see also Snedecor and Cochran, 1980). The following procedure has been therefore used.

The entire data-set has been divided into J groups and a single transformed observation, $\ln(K_s)_{i,j}$, has been expressed as:

$$\ln(K_s)_{i,j} = \mu + \tau_j + \varepsilon_{i,j} = \mu_j + \varepsilon_{i,j} \qquad j = 1, \dots, J \quad \text{and} \quad i = 1, \dots, I \tag{1}$$

with $\tau_j = \mu_j - \mu$ and with the quantities μ_j and $\varepsilon_{i,j}$ computed on the transformed data-set. On this basis, to highlight a possible absence of group effect, the null hypothesis of equality of the J values of the mean has been tested starting from the quantity SS_t defined as:

$$SS_t = \sum_i \sum_j \left(\ln(K_s)_{i,j} - \mu\right)^2 \tag{2}$$

that can be rewritten as:

$$SS_t = SS_w + SS_b = \sum_i \sum_j \left(\ln(K_s)_{i,j} - \mu_j\right)^2 + \sum_j n_j \left(\mu_j - \mu\right)^2 \tag{3}$$

where SS_w is associated to the variation within each group, SS_b to the variation between each group and the catchment, and n_j is the number of observations in each group. The sample variance, σ_t^2, the "within variance", σ_w^2, and the "between variance", σ_b^2, have been then estimated by dividing each term of Equation (3) by the corresponding degree of freedom:

$$\sigma_t^2 = \frac{SS_t}{df_t} = \frac{SS_t}{I-1} \quad (4)$$

$$\sigma_w^2 = \frac{SS_w}{df_w} = \frac{SS_w}{I-J} \quad (5)$$

$$\sigma_b^2 = \frac{SS_b}{df_b} = \frac{SS_b}{J-1} \quad (6)$$

and the variance ratio, F, has been computed as:

$$F(J-1, I-J) = \frac{\sigma_b^2}{\sigma_w^2} \quad (7)$$

For testing the null hypothesis, F has been compared to the critical value, $F_{crit}(df_b, df_w)$, obtained from an F-distribution (Snedecor and Cochran, 1980) with df_w and df_b degrees of freedom with a significance level of 5%. If F is greater than the critical value, the null hypothesis of zero group effect has to be rejected and at least one of the μ_j values is significantly different from the grand mean.

The above approach has been applied to different group ensembles: (1) ensemble obtained considering the plot locations as sources of variation to understand whether K_s variability is substantially linked to the specific physical and topographical characteristics of the measurement areas; (2) ensemble identified grouping areas with the same land use, considered because the outcomes of step (1) suggested a significant dependency of K_s variability on the plot location; (3) ensembles of plots characterized by the same land use to understand if (a) other plot-specific properties had a significant influence or (b) the observations could be considered as different sets sampled from the same population, even though collected at different locations in the catchment.

3.2 Uncertainty analysis and minimum number of samples needed

An analysis has been performed with the aim of determining the uncertainty related to the estimate of an average K_s value for a specific area. The K_s geometric mean, $\overline{K}_s$, has been chosen as the representative

estimator of the areal average saturated hydraulic conductivity. Obviously, the higher the number of measurements used to estimate the geometric mean of K_s, the higher is the confidence that the estimate is representative of the true value of $\overline{K}_s$ for the considered area. However, since the measurements are very time consuming, understanding whether it is possible to reduce the number of measurements and still obtain a reliable average, would enormously improve the planning of measurement campaigns with reduced realization times.

A well-founded uncertainty analysis based on the use of the confidence intervals has been carried out. It is rather similar to that used by Ahmed et al. (2015) with changes directed to improve the interpretation of results. The plots 2, 11-12, and 7 have been selected because they exhibited the same sampling density (about 1 measurement every 10 m^2), the same land cover (grass) but different number of observation points, i.e., 40, 20 and 9, respectively. For each data-set the non-parametric bootstrap method (Carpenter and Bithell, 2000) has been used to estimate confidence intervals around the geometric mean for different numbers of samples. The method is particularly helpful whenever confidence intervals must be calculated for small data-sets, as in the case of plot 7 where only 9 measurements are available. As suggested by Carpenter and Bithell (2000), information about the value of a population parameter (e.g. the mean, μ) can be obtained by drawing a random sample $\mathbf{Y}$ from that population and constructing an estimate $\hat{\mu}(\mathbf{Y})$ of the value of μ from that sample. The bootstrap principle is adopted to achieve information about the relationship between μ and $\hat{\mu}(\mathbf{Y})$ by looking at the relationship between $\hat{\mu}(\mathbf{y_{obs}})$ and $\hat{\mu}(\mathbf{Y}^*)$, where $\mathbf{Y}^*$ is a resample characterized by the sample of the observations $\mathbf{y_{obs}}$. Because the method involves a resampling step – which can be done assuming a specific distribution for the parameter and sampling from it (i.e. parametric bootstrap) or without assuming any distribution for the parameter and sampling with replacement (i.e. non-parametric bootstrap) – it is often used for small data-sets.

In implementing the bootstrap method, the observations have been assumed independent, sampling has been done with replacement and the process has been repeated 1000 times, as suggested for the 95% confidence interval by Carpenter and Bithell (2000). From each sub-sample the geometric mean has been estimated. A set of 1000 geometric mean values has been obtained and the 95% confidence interval has been derived by calculating the 2.5 and 97.5 percentiles. The procedure has been repeated changing the number of observations (n). For each plot, the trend of the confidence interval has been derived varying the number of

observations n from 2 to the maximum number of data available. The three trends obtained have been then normalized by the geometric mean of K_s of each plot to facilitate visual comparisons.

A further analysis has been performed using plot 2 to determine for different plot areas the minimum number of measurements requested to derive $\overline{K}_s$. This plot was the one with the largest data-set. Six sub-areas of 55, 110, 165, 215, 280 and 345 m^2 have been considered, with larger sub-areas always containing all the smaller ones. In each sub-area, 4, 5, 6, 7, 8 and 9 measurements have been drawn, and the 95% confidence intervals have been estimated as above specified for a total of 36 combinations area - sample number. Finally, the widths, A_{95}, of the confidence intervals calculated as the difference between the 97.5 and 2.5 percentiles, have been plotted against area for different sample numbers. The curves describe how the confidence in the estimation of $\overline{K}_s$ decreases when an equal number of measurements are performed on plots of increasing dimensions or how many samples are needed to obtain a given accuracy.

4 Results and Discussion

4.1 Controls on the spatial variability of saturated hydraulic conductivity

Figure 3 suggests that soil physical characteristics do not have a direct effect on K_s variability. A wider K_s variation range seems to be related to lower *om* (Figure 3a), higher *si* (Figure 3c) or lower *sa* (Figure 3d), however this may be caused by the variation of the physical characteristics with land use, rather than by a direct dependency of K_s on texture. Most likely, considering that arable areas are characterized by lower percentages of *om* and *sa*, and higher percentage of *si*, the corresponding wider variation range could be an expression of the treatment effect due to land use (investigated later), instead of a reflection of changes in soil textural composition. The weak relationship between K_s and soil textural composition is in contrast with experimental evidence of a strong connection between K_s and particle size distribution (Rahmati et al., 2018), and is likely related to the small variation of soil characteristics in the catchment. On the other hand, K_s is somewhat dependent on the slope angle (Figure 3e). In particular, higher values of K_s were observed at close to horizontal areas, while the K_s range decreases with increasing slope angle *s*. The relationship between slope angles and the textural components is shown in Figure 4. No clear dependency of *s* on any of the considered soil characteristics can be detected, therefore, the influence of *s* on K_s is not related to changing soil attributes with slope but could be due to variations in soil properties not captured by texture. In

this context differences in soil packing and presence of macropores, both influenced by random components that cannot be objectively quantified, should have generally a major role and explain also the K_s heterogeneity within each plot. On the other hand, it is not expected that the significant decrease of K_s with increasing *s*, highlighted by Morbidelli et al. (2015, 2016) under conditions of surface water moving downslope, can be deduced by measurements of K_s performed with classical devices in the absence of overland flow.

Notwithstanding the limited spatial variation of the physical and topographical soil attributes, saturated hydraulic conductivity varies substantially, with values ranging over two orders of magnitude, from a minimum of 1 mm h^{-1} to a maximum of 130 mm h^{-1} (Table 2). The high spatial variability of K_s is a well-known characteristic of this parameter, regardless of the measurement technique applied, the geographical location, the land use or the soil type (Baiamonte et al., 2017; Papanicolaou et al., 2015), therefore, this parameter is considered as a random variable depending also on random factors that cannot be quantified.

Table 2 further shows the differences in the K_s variability between arable and grassy plots. The K_s minimum and maximum observed in arable lands are significantly larger than those obtained in grassy plots with values increased more than 50%. This result can be explained by the fact that, after the harvest, i.e. the condition in which the infiltration measurements were performed, the whole root system of winter crops including stubbles was present. Therefore, the presence of the root system, typically very deep (see f.i. Thorup-Kristensen et al. (2009) for winter wheat), allowed the establishment of a preferential flow regime more efficient than that of grassy soils, where the maximum depth of the root system was much lower, with values of a few tens of centimeters (see also Brown et al., 2010; Morbidelli et al., 2014). In addition, the behavior of the arable lands is justified by the regular mixing/loosening of the plough layer that takes place twice a year, either through ploughing or chiseling, with the result that the pore size distribution can be characterized by more medium pores and less fine pores than grassland. On the other hand, the grassy plots do not exhibit a plough layer but distinct hydromorphic features more or less close to the surface. The uniform distribution of the root system that remains in the field, coupled with the periodic land management of the investigated soils, is also responsible for a more homogeneous distribution of K_s across the area. The lower variability is reflected by the coefficient of variation that in the arable fields assumes values reduced of about 25% with respect to those associated to the grassland areas. Land management operations repeated

season after season, such as tillage or plowing, in addition to a uniform land cover of crops having the same growing period and therefore similar depths of the root system appear to reduce spatial variations due to different plant varieties and soil transformation mechanisms affecting the land surface, e.g. soil compaction, crust formation or soil swelling.

A site-by-site examination reveals very similar minima of saturated hydraulic conductivity on almost every plot (Table 3). On the other hand, the maxima vary greatly between different plots. On each plot, the coefficient of variation assumes values $CV \geq 0.5$ that closely reflect the value associated to the entire catchment. This indicates that the high K_s spatial variability is still traceable when the observation plots are individually considered. More information about plot differences and similarities is provided by Figure 5, which shows the boxplots of K_s on each measurement plot. As mentioned before, the minima vary little between plots, while the maxima vary a lot. There are differences related to land use: the first quartile in grassy fields (except plot 7) is less than or equal to the minima observed on arable plots 5 and 8, indicating that at least 25% of the K_s values observed in natural conditions is lower than the minimum values observed when agricultural practices become operative. Moreover, about 50% of the K_s values observed on arable plots 5 and 8 are greater than the maximum values (excluding values that seem to be possible outliers even if for all the analyses they have been considered because included in the K_s observed range) measured on grassy plots 1, 2, 3, 6, 7 and 9 due to the fact that the median is greater than or equal to the maximum of each mentioned grassy plot. The boxplot analysis highlights a significant variability among the different measurement plots but it does not clarify if the detected variation is caused by specific physical and topographical characteristics, by different land uses or simply by the random nature of saturated hydraulic conductivity.

In order to understand whether the variability of K_s across the catchment is more related to the random nature of the parameter than to the measurement location or vice versa, an analysis of the variance has been carried out. The first step of the analysis has been therefore aimed at determining whether the plot characteristics have a significant influence on K_s spatial variability.The whole set of measurements has been divided into $J = 12$ groups, representing the twelve measurement plots. Table 4a shows the results of the analysis of variance which has been carried out on the log-transformed data. The ANOVA assumptions of normally distributed residuals and homoscedasticity have been tested with the Shapiro-Wilk test (Shapiro

and Wilk, 1965) and the Breusch-Pagan test (Breusch and Pagan, 1979), respectively. The variance between different plots, σ_b^2=4.1, is almost three times higher than the variance within each plot, σ_w^2= 1.3. This means that the largest share of variability is traceable to the physical, topographical and land cover differences between the plots. An additional evidence resides in the fact that the value of F, equal to 3.1, is greater than the critical value of 1.9, and therefore the null hypothesis of absence of treatment effect, i.e. the effect of plot location in the present case, must be rejected.

In the interest of further analyzing the origin of the treatment effect, the main variability source represented by the land use has been considered. The whole set of K_s observations has been divided into arable and grassland areas ($J = 2$), regardless of the specific type of crop cultivated in the field and the type of natural vegetation. Table 4b shows the ANOVA results when land use is considered as source of variability. The variance associated with the measurement error and the random nature of K_s, i.e. σ_w^2, is 1.4, and is thus almost negligible compared to σ_b^2= 23.7 indicating that land use is most likely the main driver for the observed K_s variations across the catchment. The value of the F-ratio of 17.2 is much larger than the critical F of 3.9 associated with a significance level of 5%, indicating that the group effect is not negligible and the means of the two groups are significantly different from each other.

Finally, since both land use and measurement plot location are responsible for a non-negligible treatment or group effect, it is interesting to understand if both factors cause saturated hydraulic conductivity to vary in space, or rather if the two are related with each other and K_s spatial variability is actually due to only one of them. In other words, we want to understand if K_s varies with plot location because of different physical and topographical soil characteristics specific of each plot or only because every plot exhibits a different land use. To this end, the whole sample of K_s observations has been split into two sub-samples – the first one consisting of measurements performed in grassland areas and the second of measurements performed in arable areas – and within each sub-sample an analysis of variance has been carried out considering as source of variation the plot location. Results of the analyses are shown in Table 4c-d. In both cases, variances associated with treatment (between) and error (within) have approximately the same values, and the F-ratio is always lower than the critical value. These results indicate that plot location does not explain the spatial variability and that measurements on different plots with the same land use can be

considered as sampled from the same population because the null hypothesis of equality of each group mean to the grand mean cannot be rejected.

The great influence of land use on the observed K_s variability is evident when two Probability Density Functions (PDFs) of K_s are associated to observations divided into the two sub-samples previously defined. Saturated hydraulic conductivity, that is usually assumed as log-normally distributed (Sharma et al., 1987; Dagan and Bresler, 1983), is characterized by the PDFs of both grassy and arable fields which tend to be bimodal but can be in any case well approximated by log-normal distributions, as tested with the Shapiro-Wilk test (Shapiro and Wilk, 1965) on the log-transformed data. In addition, as shown in Figure 6, they exhibit different shapes. In arable fields, the PDF is flatter, the peak is lower and less pronounced, the variation range is larger and the median is 34.5 mm h^{-1} as compared to 12 mm h^{-1} in grassy fields (Table 2). This means that agricultural practices and a homogeneous land cover influence the random nature of saturated hydraulic conductivity, which still varies randomly inside each group. Clearly, land use strongly influences K_s in agricultural settings and data collected in arable and grassland areas should not be considered as deriving from the same population.

4.2 Minimum number of samples for estimating areal average saturated hydraulic conductivity

The uncertainty analysis aimed at determining the minimum number of samples required for estimating a reliable K_s geometric mean, $\overline{K}_s$, for a specific area has been carried out using the data from plots 2, 11-12 and 7. These plots had the same land use, different areas (about 500 m^2, 200 m^2 and 80 m^2, respectively) and different number of total observations. However, considering that the measurements were performed with the same spatial resolution, the plots approximately had the same measurement density (about 1 observation per 10 m^2). Figure 7 shows the 95% confidence interval of $\overline{K}_s$ normalized by its geometric mean of the specific plots. For a specific number of measurements, n, the plot with smaller area results in a narrower normalized confidence interval. For example, for n=6, the width of plot 7 normalized confidence interval of 1.2 is much narrower than those of plots 2 and 11-12 (2.2 and 2.0, respectively).

Although the normalization influences the width of the confidence interval because of the different values of the geometric mean of the three plots (Table 3), it does not affect the results in terms of the

reliability exhibited by the same value of n with changing areas. Specifically, for n=6 the widths of the confidence intervals without normalization by the geometric mean have different trends (29.7, 34.8 and 21.3 mm h^{-1} for plots 7, 11-12 and 2, respectively), but the corresponding average relative errors of the geometric means of the three plots (62, 107 and 117%, respectively) confirm a higher reliability of the geometric mean estimates for smaller areas. These outcomes are likely related to the lower variability captured in grassy fields when a smaller area is sampled while, in larger areas, local soil heterogeneities (e.g. macropores, wormholes, cracks, local slope) have a higher chance to be encountered. Furthermore, the differences appear to be fairly limited if plots 11-12 and 2 are compared in terms of both the width of the normalized 95% confidence interval (Figure 7) and the average relative errors. This suggests that, beyond a certain extent, all the local soil heterogeneities characterizing the plot are captured.

This study does not involve a specific analysis of spatial correlations because of the relatively low number of samples on the smaller plots. The hypothesis of independent observations, upon which the bootstrap method is based, was adopted following Ahmed et al. (2015).

Based on the hypothesis of independent data, the confidence interval of plot 2, characterized by a sample statistically significant for the analysis of the frequency distribution, has been also computed adopting a Gaussian distribution for the log-transformed K_s data. Its trend is shown in Figure 8 together with that provided by the non-parametric bootstrap method applied to log-transformed K_s data. As expected, no significant differences can be observed.

Figure 9 shows the reduction of the confidence interval with increasing the number of measurements for the three plots. The reduction has been obtained as the difference between the width of the non-normalized confidence interval associated with n measurements and the width associated with n-1 measurements. On each plot, the reduction is large for small n. For example, if 4 measurements are used to calculate the confidence interval instead of 3, the width of the confidence interval decreases by 5, 7 and 4.3 mm h^{-1} for plots 2, 11-12 and 7, respectively. On the other hand, as n increases, the reduction decreases and tends asymptotically towards zero. This is particularly evident from the interpolated curve of plot 2, even though the same behavior is detected for plots 11-12 and 7. From this it can be deduced that the benefit – in terms of width reduction – gained by performing one extra measurement on each plot is high for small n and decreases with plot extent up to a point, specific for each plot, where the average reduction rate becomes

almost constant, i.e. the interpolated curve becomes horizontal. Therefore, the n associated with this point can be considered as the minimum number of measurements necessary to enter the "zone" where the confidence interval is stable. For example, the interpolated curve of plot 2 is almost constant for n greater than 12, suggesting that the reduction of the confidence interval width for more than 12 measurements is negligible.

A further remark concerns the possible influence of spatial correlations on the analysis. The presence of spatial correlations would have the effect of reducing the width of the confidence interval for a specific n as compared to uncorrelated data ("single realization case" of Skøien and Blöschl, 2006). The same confidence in the estimates of the geometric mean would be therefore achieved with a smaller number of observations. Consequently, the minimum number of measurements would depend on the spatial correlation structure of the investigated plot which would make the application of our results to other areas difficult. On the other hand, the assumption of independent data allows to transfer the results regardless of the plot correlation structure, even though they may represent an upper limit of the density of required measurements if correlations are present.

In order to gain insight into the relationship between grassy and arable fields in terms of accuracy in the $\overline{K}_s$ estimation, the same uncertainty analysis has been carried out on plots 5 and 7, which possess the same number of observations, the same area, but different land use. Figure 10 shows that the confidence intervals for the grassland areas are wider than for the arable areas, independently of the number of measurements n used for the derivation, which is due to the larger variability of K_s highlighted in the spatial analysis of section 4.1 for the grassland areas. This result justifies the choice of focusing the consecutive analysis only on grassy fields, because, for the same plot size, the minimum number of measurements derived for natural conditions always ensures a greater accuracy in arable environments.

In planning a field campaign one must decide the number and the location of the measurements in relation to the time required to collect a single observation and the time available. The second step of the uncertainty analysis is aimed at assisting in this choice. In order to be able to compare the combined effect of plot size and number of measurements on the accuracy of the final areal estimation of $\overline{K}_s$, six sub-plots have been derived from plot 2 in an attempt to avoid effects of temporal variation of K_s on the investigated spatial variability. Ideally, the only distinguishing aspects of the sub-plots are size and total number of

measurements available. For each sub-plot the 95% confidence intervals of $\overline{K}_s$ normalized by the geometric mean of the specific sub-plot has been generated through the non-parametric bootstrap method. The width of the normalized 95% confidence interval, A_{95}, obtained with a specific number of measurements n as a function of the plot size is shown in Figure 11. On a plot of specific dimensions, a better estimate of the average saturated hydraulic conductivity can be achieved by increasing the number of measurements in the area, in accordance with the findings of Skøien and Blöschl (2006). For example, if a plot of 165 m^2 is sampled at 5 locations, the width of the confidence interval is about twice the average K_s, but if 8 measurements are made on the same plot the width is halved (slightly less than $1 \cdot \overline{K}_s$), i.e. the reliability associated with the $\overline{K}_s$ estimation is almost doubled. On the other hand, when the same number of samples is taken in increasing areas, the width of the confidence interval increases as well, indicating how the samples progressively lose the ability of representing the true value of $\overline{K}_s$. If 7 measurements are performed over an area of 110 m^2, the width of the confidence interval is $1.1 \cdot \overline{K}_s$, but the uncertainty almost doubles whenever the same number of samples is taken on a plot of 345 m^2 ($A_{95} = 2.1 \cdot \overline{K}_s$).

As mentioned before, the confidence intervals are obtained with the non-parametric bootstrap method which is based on the hypothesis of independent data. Although the increase in uncertainty with increasing areas could be partially due to a progressive decorrelation, this is not the case because in the derivation of the confidence intervals spatial correlations are not considered. One possible explanation may be the increased likelihood of encountering soil local heterogeneities in larger areas. Additionally, if one considers a sub-area of plot 2 of 120 m^2 the contained measured K_s are characterized by a variance of about 170 $mm^2\ h^{-2}$. When the sub-area is extended up to 300 m^2 the variance increases as well and it is equal to 350 $mm^2\ h^{-2}$. Finally, if the sub-area is further extended up to 450 m^2 the variance reaches the value of 410 $mm^2\ h^{-2}$, and for greater areas the variance value fluctuates in the range 350 – 400 $mm^2\ h^{-2}$. This trend confirms that when the sampled area increases more variability is encountered and therefore the uncertainty on the estimation of the K_s geometric mean value increases as well.

Figure 11 is also useful to derive a minimum number of samples that have to be taken in an area of specific dimensions for a tradeoff between accuracy (or uncertainty) and time required for the measurements. Selection of the accuracy level should consider the typical $\overline{K}_s$ value of the study since the average error is relative to it. For example, if A_{95} is assumed equal to 1.5 for a silty loam soil, for which a typical K_s value of

about 1.6 mm h^{-1} is expected (Corradini et al., 1997), the estimated value of $\overline{K}_s$ can vary on average between 0.4 and 2.8 mm h^{-1}. However, if the same width is chosen for a sandy loam soil, for which a typical K_s value of about 25 mm h^{-1} is expected (Corradini et al., 1997), the estimated value of $\overline{K}_s$ will vary on average between 6.25 and 43.75 mm h^{-1}. Furthermore, the level of accuracy should be selected in relation to the final purpose of the measurement campaign. For instance, if the peak discharge of a stream has to be estimated by a rainfall-runoff model for designing a weir system along the stream, the required accuracy of $\overline{K}_s$ could be inferred from the required accuracy of the flood estimate by error propagation.

The accuracy level suggested by Ahmed et al. (2015) varies in the range of 1.8-2.2. When the reference value is taken as 1.8, Figure 11 suggests that for a plot of 110 m^2 at least 5 measurements are needed to obtain a width of the normalized 95% confidence interval equal to or smaller than the reference value. Similarly, on a plot of 280 m^2 at least 8 samples should be taken in order to estimate average saturated hydraulic conductivity.

5 Conclusions

In this study 131 saturated hydraulic conductivity measurements were performed in a small Austrian watershed with double-ring infiltrometers. This device was chosen due to the measurement repeatability, low cost, which allowed parallel measurements, and ease of installation and operation in natural environments. Measurements were carried out on 12 plots, with a 3 m spatial resolution, trying to avoid local macroporosity and preferential flow paths as well as agricultural machinery tracks. Observations were collected in both grassland and arable areas to account for land cover effects on the variability of K_s.

While soil texture is not significantly variable in the catchment, K_s varies by two orders of magnitude, with a minimum of 1 mm h^{-1} and a maximum of 130 mm h^{-1}. The variation range in arable areas is wider than in grassland (pasture, forest) areas. The minima are similar, but the maximum value of K_s in cultivated plots is 50% greater than those in the grassy plots. Soil management practices and uniform land cover are considered the main causes of the lower spatial variability of $K_s$in the cultivated areas, where CV assumes values reduced of about 25% with respect to those obtained in the areas with natural vegetation.

An analysis of variance has been also carried out with the purpose of understanding the role of plot characteristics, including land cover, on the variability of saturated hydraulic conductivity. The results show

that the main control is the land cover and the plot location influences K_s only because different plots are characterized by different land uses. The great influence of land cover is also reflected by the probability density functions considered separately for grassland and arable areas. Although both PDFs follow a log-normal distribution, their shapes are rather different, with a median of 12 mm h^{-1} in grassy fields and 34.5 mm h^{-1} in arable fields. Therefore, two separate PDFs should be considered to characterize the probability distribution of K_s measurements performed with a double-ring infiltrometer in natural or agricultural settings.

Finally, an uncertainty analysis has been performed aimed at determining the minimum number of measurements necessary for estimating the geometric mean of K_s for a specific area. From the analysis of three grassy plots with the same measurement density, it is clear that the uncertainty, expressed in terms of width reduction of the 95% confidence interval, decreases rapidly as the number of measurements increases up to a certain value. Here the reduction stabilizes and, after this point, the increasing of the number of observations used in the estimate provides little benefit in accuracy compared to the cost, in terms of time and resources, of each additional measurement. The width of the confidence interval obtained with a specific number of measurements increases with plot size most likely because of the higher chance to encounter soil local heterogeneities such as macropores, wormholes, different root systems or preferential flow paths. The increase appears to be limited beyond a certain extent, suggesting that all the local soil heterogeneities characterizing the plot are captured, even though further analyses on this should be made.

The chart of the confidence interval width as a function of number of measurements and plot size can be used as a support in sampling design to obtain a reliable $\overline{K}_s$ with the minimum number of samples.

The chart could be also used for estimating the minimum number of DRI measurements in other catchments that exhibit geo-morphological characteristics similar to those characterizing this study, i.e. an agricultural setting, slope angles less than 10° and silty soils. If spatial correlations of K_s are present, the proposed procedure represents an upper limit of the uncertainty to be expected. Finally, the methodology adopted here could be of interest to develop similar investigations in different areas.

A limitation of this work is that the K_s measurements through the catchment were not performed at the same time. Therefore a distortion of the spatial pattern of K_s cannot be ruled out because of possible changes of the local values. This is a problem that cannot be completely solved, at least considering the limits of the

currently available devices, and that in any case should not have significantly affected the main features of the K_s spatial variability field obtained in this study.

Acknowledgements

The authors would like to acknowledge financial support provided by the Austrian Science Funds (FWF) as part of the Vienna Doctoral Programme on Water Resource Systems (DK W1219-N22) and the Italian Ministry of Education, University and Research (PRIN 2015).

References

Ahmed, F., Nestingen, R., Nieber, J.L., Gulliver, J.S., Hozalski, R.M. 2014. A modified Philip-Dunne infiltrometer for measuring the field-saturated hydraulic conductivity of surface soil. Vadose Zone J. 13(10), doi:10.2136/vzj2014.01.0012.

Ahmed, F., Gulliver, J., Nieber, J., 2015. Field infiltration measurements in grassed roadside drainage ditches: Spatial and temporal variability. J. Hydrol. 530, 604-611, https://doi.org/10.1016/j.jhydrol.2015.10.012.

Alletto, L., Coquet, Y., 2009. Temporal and spatial variability of soil bulk density and near-saturated hydraulic conductivity under two contrasted tillage management systems. Geoderma 152(1-2), 85-94, https://doi.org/10.1016/j.geoderma.2009.05.023.

Armstrong, R., Slade, S., Eperjesi, F., 2000. An introduction to analysis of variance (ANOVA) with special reference to data from clinical experiments in optometry. Ophthal. Physl. Opt. 20(3), 235-241, https://doi.org/10.1046/j.1475-1313.2000.00502.x.

Assouline, S., Mualem, Y., 2002. Infiltration during soil sealing: The effect of areal heterogeneity of soil hydraulic properties. Wat. Resour. Res. 38(12), 1286.

Assouline, S., Mualem, Y., 2006. Runoff from heterogeneous small bare catchments during soil surface sealing. Wat. Resour. Res. 42, W12405.

Bagarello, V., Iovino, M., Elrick, D., 2004. A Simplified Falling-Head Technique for Rapid Determination of Field-Saturated Hydraulic Conductivity. Soil Scie. Soc. Am. J., 68(1), 66-73.

Bagarello, V., Baiamonte, G., Castellini, M., Di Prima, S., Iovino, M., 2014a. A comparison between the single ring pressure infiltrometer and simplified falling head techniques. Hydrol. Process. 28(18), 4843-4853, https://doi.org/10.1002/hyp.9980.

Bagarello, V., Di Prima, S., Iovino, M. 2014b. Comparing alternative algorithms to analyze the beerkan infiltration experiment. Soil Scie. Soc. Am. J., 78(3), 724-736

Baiamonte, G., Bagarello, V., D'Asaro, F., Palmeri, V., 2017. Factors Influencing Point Measurement of Near-surface Saturated Soil Hydraulic Conductivity in a Small Sicilian Basin. Land Degrad. Dev. 28(3), 970-982, https://doi.org/10.1002/ldr.2674.

Blöschl, G., Sivapalan, M., 1995. Scale issues in hydrological medelling: A review. Hydrol. Process. 9(3-4), 251-290, https://doi.org/10.1002/hyp.3360090305.

Blöschl, G., Blaschke, A., Broer, M., Bucher, C., Carr, G., Chen, X., Eder, A., Exner-Kittridge, M., Farnleitner, A., Flores-Orozco, A., Haas, P., Hogan, P., Kazemi Amiri, A., Oismüller, M., Parajka, J., Silasari, R., Stadler, P., Strauss, P., Vreugdenhil, M., Wagrner, W., Zessner, M., 2016. The Hydrological Open Air Laboratory (HOAL) in Petzenkirchen: A hypothesis-driven observatory. Hydrol. Earth Syst. Sc. 20(1), 227-255, https://doi.org/10.5194/hess-20-227-2016.

Bonell, M., Purandara, B.K., Venkatesh, B., Krishnaswamy, J., Acharya, H.A.K., Singh, U.V., Jayakumar, R., Chappell, N., 2010. The impact of forest use and reforestation on soil hydraulic conductivity in the Western Ghats of India: Implications for surface and sub-surface hydrology. J. Hydrol. 391(1-2), 47-62, https://doi.org/10.1016/j.jhydrol.2010.07.004.

Bouma J. (1989) Using Soil Survey Data for Quantitative Land Evaluation. In: Stewart B.A. (eds) Advances in Soil Science. Advances in Soil Science (9), 177-213. Springer, New York, NY, https://doi.org/10.1007/978-1-4612-3532-3_4.

Bouma, J., Droogers, P., Sonneveld, M.P.W., Ritsema, C.J., Hunink, J.E., Immerzeel, W.W. Kauffman, S., 2011. Hydropedological insights when considering catchment classification. Hydrol. Earth Syst. Sc. 15(6), 1909–1919, https://doi.org/10.5194/hess-15-1909-2011.

Breusch, T., Pagan, A., 1979. A Simple Test for Heteroscedasticity and Random Coefficient Variation. Econometrica 47(5), 1287, https://doi.org/10.2307/1911963.

Brown, R., Percivalle, C., Narkiewicz, S., DeCuollo, S., 2010. Relative rooting depths of native grasses and amenity grasses with potential for use on roadsides in New England. HortScience 45(3), 393-400.

Carpenter, J., Bithell, J., 2000. Bootstrap confidence intervals: When, which, what? A practical guide for medical statisticians. Stat. Med. 19(9), 1141-1164.

Corradini, C., Melone, F., Smith, R.E., 1997. A unified model for infiltration and redistribution during complex rainfall patterns. J. Hydrol. 192(1-4), 104-124.

Corradini, C., Flammini, A., Morbidelli, R., Govindaraju, R., 2011. A conceptual model for infiltration in two-layered soils with a more permeable upper layer: From local to field scale. J. Hydrol. 410(1-2), 62-72, https://doi.org/10.1016/j.jhydrol.2011.09.005.

Dagan, G., Bresler, E., 1983. Unsaturated flow in spatially variable fields 1.Derivation of Model of Infilteration and Redistribution. Wat. Resour. Res. 19(2), 413-420.

Dexter, A., Czyz, E., Gaţe, O., 2004. Soil structure and the saturated hydraulic conductivity of subsoils. Soil Till. Res. 79(2), 185-189, https://doi.org/10.1016/j.still.2004.07.007.

Essig, E., Corradini, C., Morbidelli, R., Govindaraju, R., 2009. Infiltration and deep flow over sloping surfaces: Comparison of numerical and experimental results. J. Hydrol. 374(1-2), 30-42, https://doi.org/10.1016/j.jhydrol.2009.05.017.

Flammini, A., Morbidelli, R., Saltalippi, C., Picciafuofo, T., Corradini, C., Govindaraju, R.S., 2018. Reassessment of a semi-analytical field-scale infiltration model through experiments under natural rainfall events. J. Hydrol. 565, 835-845.

Govindaraju, R., Corradini, C., Morbidelli, R., 2012. Local- and field-scale infiltration into vertically non-uniform soils with spatially-variable surface hydraulic conductivities. Hydrol. Process. 26(21), 3293-3301, https://doi.org/10.1002/hyp.8454.

Hu, W., She, D., Shao, M., Chun, K., Si, B., 2015. Effects of initial soil water content and saturated hydraulic conductivity variability on small watershed runoff simulation using LISEM. Hydrolog. Sci. J. 60(6), 1137-1154, https://doi.org/10.1080/02626667.2014.903332.

Jabro, J., 1992. Estimation of Saturated Hydraulic Conductivity of Soils From Particle Size Distribution and Bulk Density Data. T. ASAE 35(2), 557-560, https://doi.org/10.13031/2013.28633.

Lai, J., Ren, L., 2007. Assessing the Size Dependency of Measured Hydraulic Conductivity Using Double-Ring Infiltrometers and Numerical Simulation. Soil Sci. Soc. Am. J. 71(6), 1667-1675, https://doi.org/10.2136/sssaj2006.0227.

Lassabatère, L., Angulo-Jaramillo, R., Soria Ugalde, J., Cuenca, R., Braud, I., Haverkamp, R., 2006. Beerkan Estimation of Soil Transfer Parameters through Infiltration Experiments-BEST. Soil Sci. Soc. Am. J. 70(2), 521-532, https://doi.org/10.2136/sssaj2005.0026.

Loague, K., Gander, G.A., 1990. R-5 revisited, 1, Spatial variability of infiltration on a small rangeland catchment. Water Resour. Res. 26(5), 957-971.

Mohanty, B., Ankeny, M., R., H., Kanwar, R., 1994. Spatial analysis of hydraulic conductivity measured using disc infiltrometer. Water Resour. Res. 30(9)(9), 2489-2498.

Morbidelli, R., Saltalippi, C., Flammini, A., Rossi, E., Corradini, C., 2014. Soil water content vertical profiles under natural conditions: Matching of experiments and simulations by a conceptual model. Hydrol. Process. 28(17), 4732-4742.

Morbidelli, R., Saltalippi, C., Flammini, A., Cifrodelli, M., Corradini, C., Govindaraju, R., 2015. Infiltration on sloping surfaces: Laboratory experimental evidence and implications for infiltration modeling. J. Hydrol. 523, 79-85, https://doi.org/10.1016/j.jhydrol.2015.01.041.

Morbidelli, R., Saltalippi, C., Flammini, A., Cifrodelli, M., Picciafuoco, T., Corradini, C., Govindaraju, R., 2016. Laboratory investigation on the role of slope on infiltration over grassy soils. J. Hydrol. 543, 542-547, https://doi.org/10.1016/j.jhydrol.2016.10.024.

Morbidelli, R., Saltalippi, C., Flammini, A., Cifrodelli, M., Picciafuoco, T., Corradini, C., Govindaraju, R., 2017. In-Situ Measurements of Soil Saturated Hydraulic Conductivity: Assessment of Reliability through Rainfall-Runoff Experiments. Hydrol. Process. 31(17), 3084-3094, https://doi.org/10.1002/hyp.11247.

Papanicolaou, A., Elhakeem, M., Wilson, C.G., Lee Burras, C., West, L.T., Lin, H., Clark, B., Oneal, B.E., 2015. Spatial variability of saturated hydraulic conductivity at the hillslope scale: Understanding the role of land management and erosional effect. Geoderma 243-244, 58-68, https://doi.org/10.1016/j.geoderma.2014.12.010.

Parlange, J.-Y., Lisle, I., Braddock, R., Smith, R., 1982. The three-parameter infiltration equation. Soil Sci. 133(6), 337-341.

Perroux, K.M. White, I., 1988. Designs for disc permeameters. Soil Sci. Soc. Am. J. 52(5), 1205-1215.

Philip, J., 1991. Hillslope infiltration: Planar slopes. Water Resour. Res. 27(1), 109-117, https://doi.org/10.1029/90WR01704.

Rahmati, M., Weihermüller, L., Vanderborght, J., Pachepsky, Y. A., Mao, L., Sadeghi, S. H., Moosavi, N., Kheirfam, H., Montzka, C., Van Looy, K., Toth, B., Hazbavi, Z., Al Yamani, W., Albalasmeh, A. A., Alghzawi, M. Z., Angulo-Jaramillo, R., Antonino, A. C. D., Arampatzis, G., Armindo, R. A., Asadi, H., Bamutaze, Y., Batlle-Aguilar, J., Béchet, B., Becker, F., Blöschl, G., Bohne, K., Braud, I., Castellano, C., Cerdà, A., Chalhoub, M., Cichota, R., Císlerová, M., Clothier, B., Coquet, Y., Cornelis, W., Corradini, C., Coutinho, A. P., de Oliveira, M. B., de Macedo, J. R., Durães, M. F., Emami, H., Eskandari, I., Farajnia, A., Flammini, A., Fodor, N., Gharaibeh, M., Ghavimipanah, M. H., Ghezzehei, T. A., Giertz, S., Hatzigiannakis, E. G., Horn, R., Jiménez, J. J., Jacques, D., Keesstra, S. D., Kelishadi, H., Kiani-Harchegani, M., Kouselou, M., Kumar Jha, M., Lassabatere, L., Li, X., Liebig, M. A., Lichner, L., López, M. V., Machiwal, D., Mallants, D., Mallmann, M. S., de Oliveira Marques, J. D., Marshall, M. R., Mertens, J., Meunier, F., Mohammadi, M. H., Mohanty, B. P., Pulido-Moncada, M., Montenegro, S., Morbidelli, R., Moret-Fernández, D., Moosavi, A. A., Mosaddeghi, M. R., Mousavi, S. B., Mozaffari, H., Nabiollahi, K., Neyshabouri, M. R., Ottoni, M. V., Ottoni Filho, T. B., Pahlavan-Rad, M. R., Panagopoulos, A., Peth, S., Peyneau, P.-E., Picciafuoco, T., Poesen, J., Pulido, M., Reinert, D. J., Reinsch, S., Rezaei, M., Roberts, F. P., Robinson, D., Rodrigo-Comino, J., Rotunno Filho, O. C., Saito, T., Suganuma, H., Saltalippi, C., Sándor, R., Schütt, B., Seeger, M., Sepehrnia, N., Sharifi Moghaddam, E., Shukla, M., Shutaro, S., Sorando, R., Stanley, A. A., Strauss, P., Su, Z., Taghizadeh-Mehrjardi, R., Taguas, E., Teixeira, W. G., Vaezi, A. R., Vafakhah, M., Vogel, T., Vogeler, I., Votrubova, J., Werner, S., Winarski, T., Yilmaz, D., Young, M. H., Zacharias, S., Zeng, Y., Zhao, Y., Zhao, H., Vereecken, H., 2018. Development and analysis of the Soil Water Infiltration Global database. Earth Syst. Sci. Data 10, 1237-1263, https://doi.org/10.5194/essd-10-1237-2018.

Reynolds, W., Erlick, D., 1985. in Situ Measurement of Field-Saturated Hydraulic Conductivity, Sorptivity, and the A-Parameter Using the Guelph Permeameter. Soil Sci. 140(4), 292-302.

Reynolds, W.D., Bowman, B.T., Brunke, R.R., Drury, C.F., Tan, C.S., 2000. Comparison of tension infiltrometer, pressure infiltrometer and soil core estimates of saturated hydraulic conductivity. Soil Sci. Soc. Am. J. 64, 478-484.

Saxton, K., Rawls, W., Romberger, J., Papendick, R., 1986. Estimating Generalized Soil-water Characteristics from Texture. Soil Sci. Soc. Am. J. 50(4), 1031-1036, https://doi.org/10.2136/sssaj1986.03615995005000040039x.

Shapiro, S., Wilk, M., 1965. An Analysis of Variance Test for Normality (Complete Samples). Biometrika 52(3/4), 591-611, https://doi.org/10.2307/2333709.

Sharma, M., Barron, R., Fernie, M., 1987. Areal distribution of infiltration parameters and some soil physical properties in lateritic catchments. J. Hydrol. 94(1-2), 109-127, https://doi.org/10.1016/0022-1694(87)90035-7.

Skøien, J.O., Blöschl, G., 2006. Sampling scale effects in random fields and implications for environmental monitoring. Environ. Monit. Assess. 114 (1-3), 521-552, https://doi.org/10.1007/s10661-006-4939-z.

Smith, R., Goodrich, D., 2000. Model For Rainfall Excess Patterns on Randomly Heterogeneous Areas. J. Hydrol. Eng. 5(4), 355-362, https://doi.org/10.1061/(ASCE)1084-0699(2000)5:4(355).

Snedecor, G., Cochran, W., 1980. Statistical Methods (7th ed.). Iowa State University Press.

Sobieraj, J., Elsenbeer, H., Cameron, G., 2004. Scale dependency in spatial patterns of saturated hydraulic conductivity. Catena 55(1), 49-77, https://doi.org/10.1016/S0341-8162(03)00090-0.

Swartzendruber, D., Olson, T., 1961. Model study of the double-ring infiltrometer as affected by depth of wetting and particle size. Soil Sci. 92(4), 219-225, https://doi.org/10.1097/00010694-196110000-00001.

Taskinen, A., Sirviö, H., Bruen, M., 2008. Statistical analysis of the effects on overland flow of spatial variability in soil hydraulic conductivity. Hydrolog. Sci. J. 53(2), 387-400, https://doi.org/10.1623/hysj.53.2.387.

Thorup-Kristensen, K., Cortasa, M., Loges, R., 2009. Winter wheat roots grow twice as deep as spring wheat roots, is this important for N uptake and N leaching losses? Plant and Soil 322(1), 101-114, https://doi.org/10.1007/s11104-009-9898-z.

Tossell, R., Dickinson, W., Rudra, R., Wall, G., 1987. A portable rainfall simulator. Can. Agr. Eng. 29(2), 155-162.

Verbist, K., Cornelis, W., Torfs, S., Gabriels, D., 2013. Comparing Methods to Determine Hydraulic Conductivities on Stony Soils. Soil Sci. Soc. Am. J. 77(1), 25-42, https://doi.org/10.2136/sssaj2012.0025.

Vieira, S., Nielsen, D., Biggar, J., 1981. Spatial Variability of Field-Measured Infiltration Rate. Soil Sci. Soc. Am. J. 45(6), 1040-1048, https://doi.org/10.2136/sssaj1981.03615995004500060007x.

Woolhiser, D., Smith, R., Giraldez, J., 1996. Effects of spatial variability of saturated hydraulic conductivity on Hortonian overland flow. Water Resour. Res. 32(3), 671-678, https://doi.org/10.1029/95WR03108.

List of tables

Table 1 – General statistics of the physical and topographic soil characteristics available in the same locations where the infiltration measurements were performed. Min = minimum value; Max = maximum value; Mean = arithmetic mean; CV = coefficient of variation; *om* = organic matter content; *cl* = clay content; *si* = silt content (as complementary to 100% of clay and sand); *sa* = sand content; *s* = slope angle; *el* = elevation.

Table 2 – General statistics of the K_s values measured with double-ring infiltrometer. Min = minimum value; Max = maximum value; Mean = arithmetic mean; CV = coefficient of variation; Skew = skewness; Mean log = arithmetic mean of the log-transformed values; CV log = coefficient of variation of the log-transformed values; Arable land = K_s values measured in arable areas; Grassland = K_s values measured in grassy areas; Total = all K_s values.

Table 3 – General statistics of the K_s values, grouped by plot. n. obs. = number of observations in each plot; Min = minimum value; Max = maximum value; Mean = arithmetic mean; CV = coefficient of variation; G.mean = geometric mean.

Table 4 – Results of ANOVA analyses. df = degree of freedom ($df_b; df_w; df_t$); SS = sums of squares ($SS_b; SS_w; SS_t$); σ^2 = variance ($\sigma_b^2; \sigma_w^2$); F = variance ratio; F_{crit} = critical value of the F-ratio. All variances (SS, σ^2) relate to the logarithms of K_s.

List of figures

Figure 9 – Reduction of the width of the non-normalized confidence interval of the saturated hydraulic conductivity geometric mean obtained using one extra measurement in the bootstrap method. For a specific *n* the corresponding point represents the difference between the width associated with *n* measurements and with *n-1* measurements.

Figure 10 – Normalized 95% confidence intervals by the K_s geometric mean, obtained via the non-parametric bootstrap method for a grassy and an arable plot. The x-axis represents the number of measurements used for each plot.

Figure 11 – Width of the 95% confidence intervals normalized by the saturated hydraulic conductivity, K_s, geometric mean plotted against plot size. Lines represent the number of measurements used for the evaluation of the confidence interval and the geometric mean.

Tables

Table 1 – General statistics of the physical and topographic soil characteristics available in the same locations where the infiltration measurements were performed. Min = minimum value; Max = maximum value; Mean = arithmetic mean; CV = coefficient of variation; *om* = organic matter content; *cl* = clay content; *si* = silt content (as complementary to 100% of clay and sand); *sa* = sand content; *s* = slope angle; *el* = elevation.

Statistics	*om* (%)	*cl* (%)	*si* (%)	*sa* (%)	*s* (°)	*el* (m a.s.l.)
Min	1.9	17.6	68.7	6.0	2.4	263.1
Max	3.4	23.0	73.8	11.5	13.0	316.4
Mean	2.6	20.3	71.3	8.4	6.1	279.3
St. dev.	0.4	1.1	1.5	1.2	1.9	16.3
CV (%)	13.8	5.6	2.1	14.7	31.7	5.8

Table 2 – General statistics of the K_s values measured with double-ring infiltrometer. Min = minimum value; Max = maximum value; Mean = arithmetic mean; CV = coefficient of variation; Skew = skewness; Mean log = arithmetic mean of the log-transformed values; CV log = coefficient of variation of the log-transformed values; Arable land = K_s values measured in arable areas; Grassland = K_s values measured in grassy areas; Total = all K_s values.

Statistics	Arable land	Grassland	Total
Min (mm h^{-1})	2.0	1.0	1.0
Max (mm h^{-1})	130.0	84.0	130.0
Mean (mm h^{-1})	46.9	20.2	25.1
St. dev. (mm h^{-1})	35.5	20.3	25.8
CV (%)	75.6	100.3	102.7
Skew (-)	0.8	1.1	1.5
Median (mm h^{-1})	34.5	12.0	15.0
Mean log (-)	3.5	2.4	2.6
CV log (%)	27.7	50.6	47.9

Table 3 – General statistics of the K_s values, grouped by plot. n. obs. = number of observations in each plot; Min = minimum value; Max = maximum value; Mean = arithmetic mean; CV = coefficient of variation; G.mean = geometric mean.

Plot	1	2	3	4	5	6	7	8	9	10	11	12
n. obs.	8	40	4	9	9	8	9	6	9	9	10	10
Min (mm h^{-1})	1.5	1.0	6.0	2.0	18.0	2.0	3.0	12.0	1.8	3.0	3.0	2.0
Max (mm h^{-1})	12.0	78.0	42.0	87.0	118.5	46.5	48.0	130.0	58.5	66.0	54.0	84.0
Mean (mm h^{-1})	5.8	17.0	23.6	35.7	51.8	18.4	30.3	56.4	16.0	22.9	20.2	36.8
St. dev. (mm h^{-1})	3.5	18.6	18.8	28.2	32.2	16.7	15.1	49.8	18.5	28.7	19.7	26.6
Median (mm h^{-1})	5.3	12.0	23.3	22.5	51.0	12.8	34.5	45.8	7.0	4.0	12.0	40.5
CV (%)	60.8	109.0	79.4	78.9	62.2	90.6	49.8	88.3	115.7	125.3	97.6	72.2
G.mean (mm h^{-1})	4.8	9.1	17.1	23.4	43.5	12.3	24.0	36.6	8.9	9.4	11.5	22.7

Table 4 – Results of ANOVA analyses. df = degree of freedom (df_b; df_w; df_t); SS = sums of squares (SS_b; SS_w; SS_t); σ^2 = variance (σ_b^2; σ_w^2); F = variance ratio; F_{crit} = critical value of the F-ratio. All variances (SS, σ^2) relate to the logarithms of K_s.

(a) All measurements grouped by plot

Source of variation	df	SS	σ^2	F	F_{crit}
Plot (between)	11	44.7	4.1	3.1	1.9
Error (within)	119	156.9	1.3		
Total	130	201.5			

(b) All measurements grouped by land use

Source of variation	df	SS	σ^2	F	F_{crit}
Land use (between)	1	23.7	23.7	17.2	3.9
Error (within)	129	177.8	1.4		
Total	130	201.5			

(c) Grassland measurements grouped by plot

Source of variation	df	SS	σ^2	F	F_{crit}
Plot (between)	8	19.1	2.4	1.7	2.0
Error (within)	98	137.0	1.4		
Total	106	156.2			

(d) Arable land measurements grouped by plot

Source of variation	df	SS	σ^2	F	F_{crit}
Plot (between)	2	1.8	0.9	1.0	3.5
Error (within)	21	19.9	0.9		
Total	23	21.7			

Figures

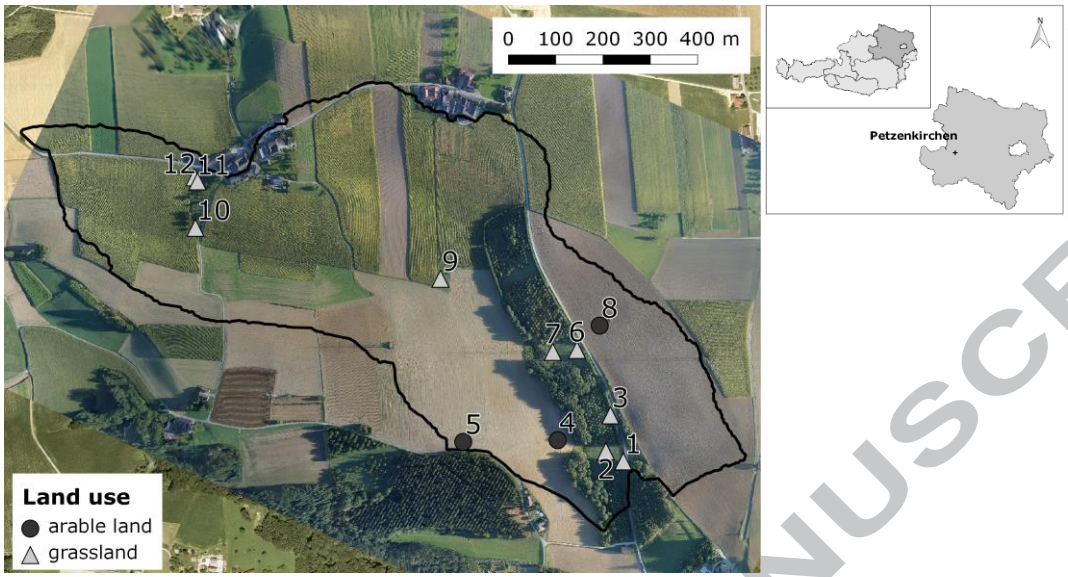

Figure 1 – Measurement plots in the catchment. Dark-grey circles represent plots located in arable areas, light-grey triangles represent plots located in grassland areas. The catchment location in the Lower Austria region is also shown.

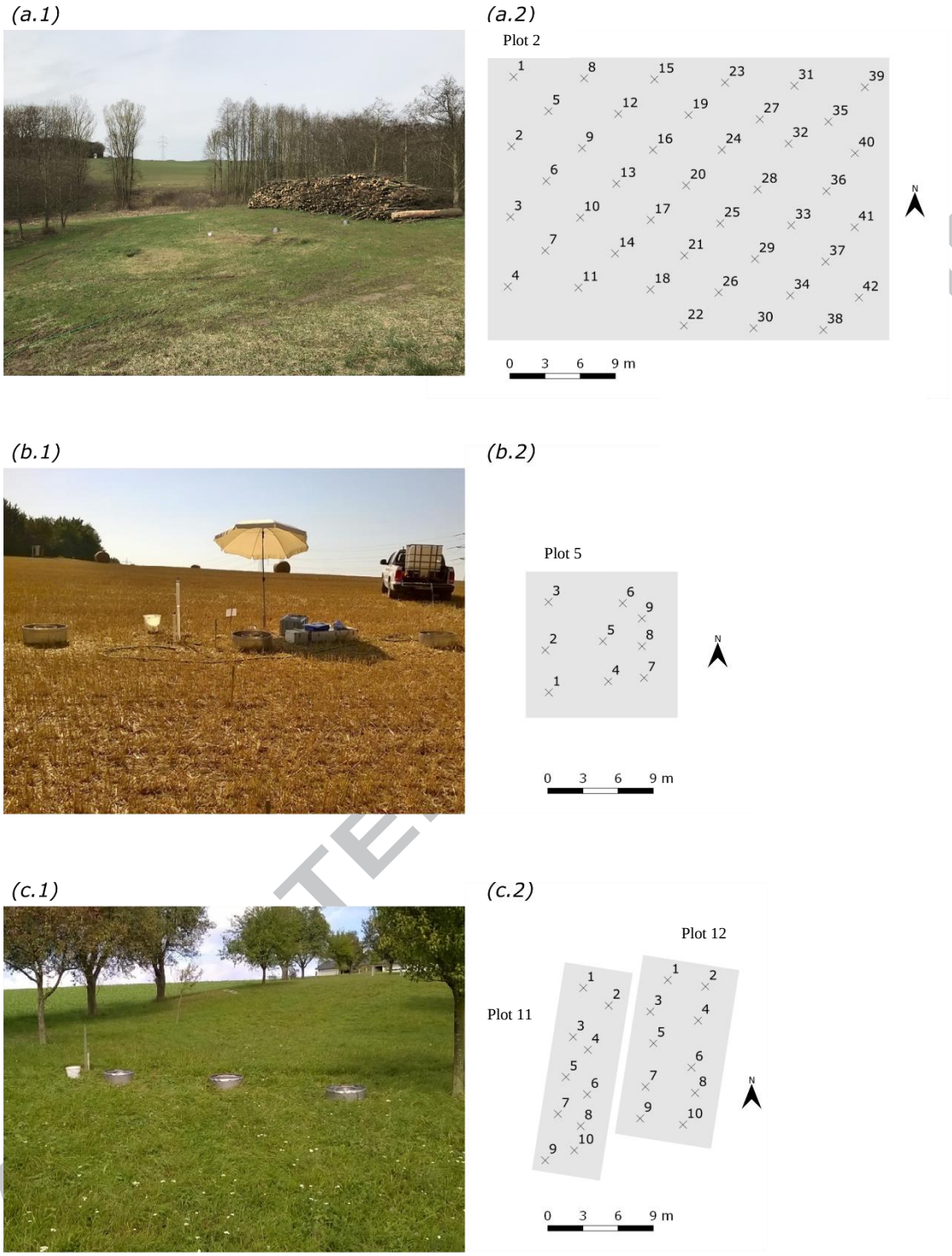

Figure 2 – Pictures of some measurement sites (1) and correspondent scheme of measurements performed (2) for different environmental conditions present in the plots: (a) plot 2, the largest plot located in the proximity of the forested area of the catchment and featuring a grassy meadow land; (b) plot 5, located in the cultivated area of the catchment; (c) plots 11 and 12, both located in a naturally vegetated orchard.

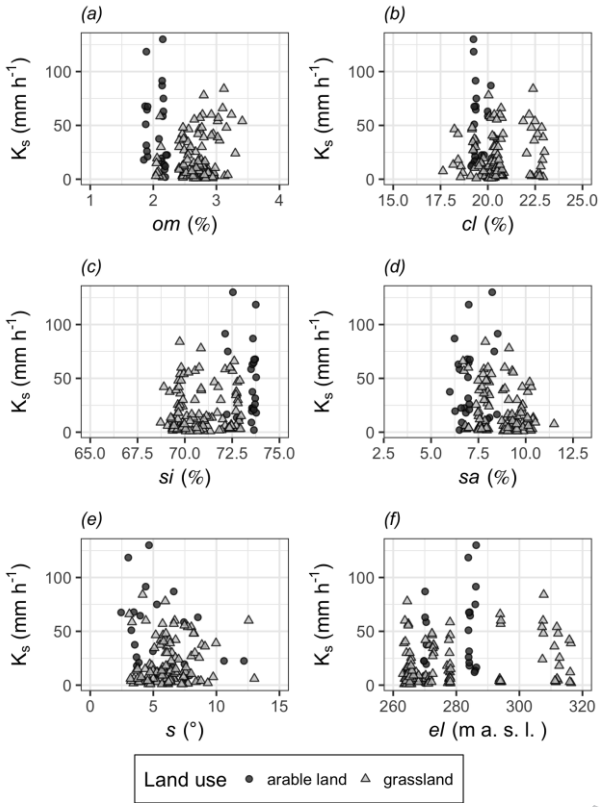

Figure 3 – Saturated hydraulic conductivity, K_s, observations plotted against (a) organic matter content, *om*; (b) clay content, *cl*; (c) silt content, *si*; (d) sand content, *sa*; (e) slope angle, *s*; (f) elevation, *el*. Dark-grey circles represent plots located in arable areas, light-grey triangles represent plots located in grassland areas.

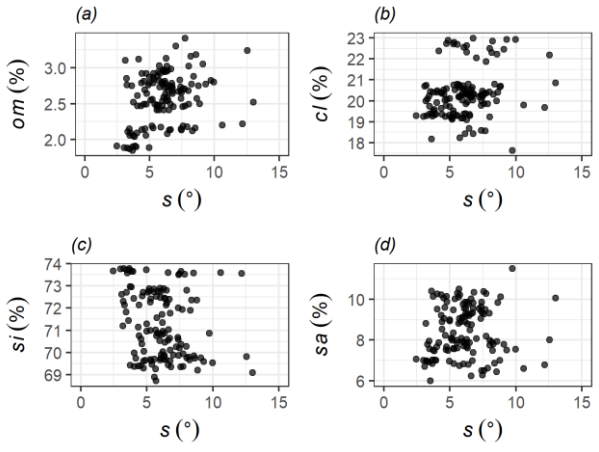

Figure 4 – Slope angles plotted against (a) organic matter content, *om*; (b) clay content, *cl*; (c) silt content, *si*; (d) sand content, *sa*.

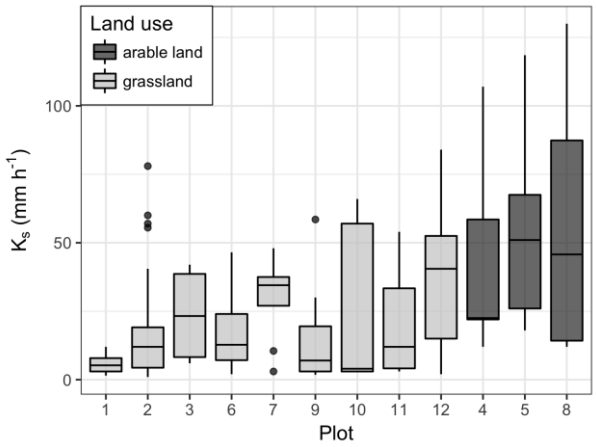

Figure 5 – Boxplots of saturated hydraulic conductivity, K_s, for the different measurement plots. Dark-grey boxplots represent plots located in arable areas, light-grey boxplots represent plots located in grassland areas. The box represents the interquartile range, i.e. difference between the third and the first quartiles. The horizontal black line represents the median of each plot. The dark-grey dots, usually representing possible outliers, were nevertheless considered as acceptable occurrences of K_s as they lie in the typical K_s domain.

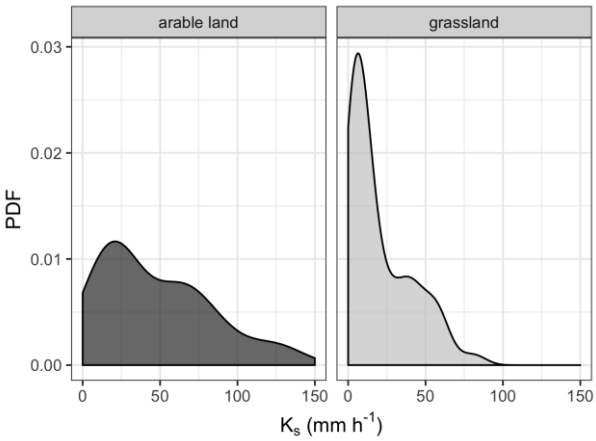

Figure 6 – Probability Density Functions (PDFs) of observed saturated hydraulic conductivity, K_s, values on both arable (dark-grey) and grassy (light-grey) fields.

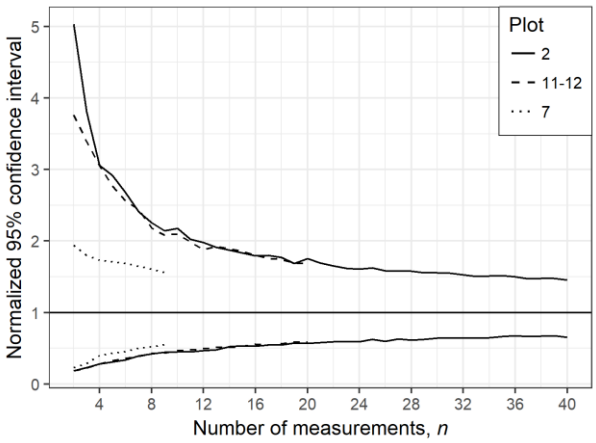

Figure 7 – Normalized 95% confidence intervals of the saturated hydraulic conductivity geometric mean K_s obtained via non-parametric bootstrap method for 3 grassy plots.

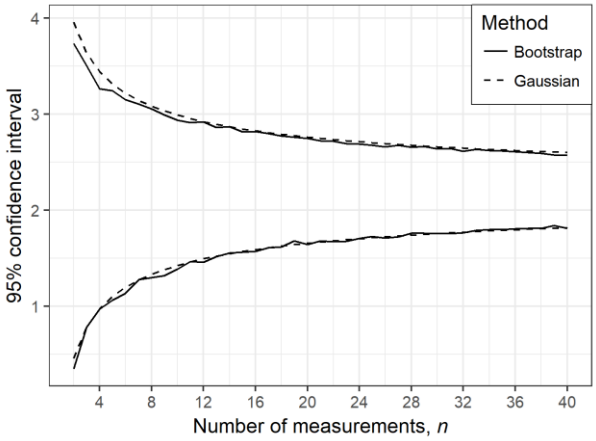

Figure 8 – 95% confidence interval of the saturated hydraulic conductivity geometric mean obtained applying the non-parametric bootstrap method (solid curve) and for a Gaussian variable (dashed curve). Plot 2, log-transformed data.

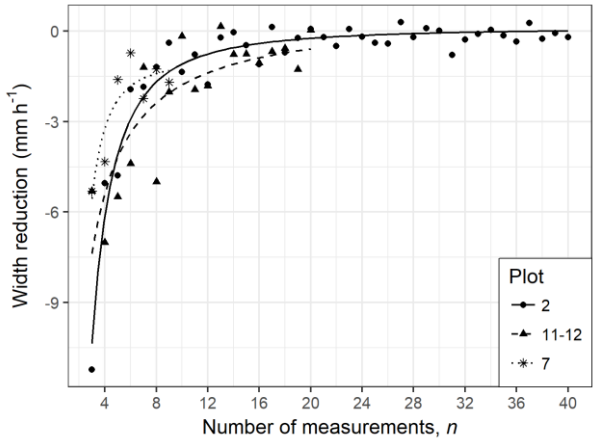

Figure 9 – Reduction of the width of the non-normalized confidence interval of the saturated hydraulic conductivity geometric mean obtained using one extra measurement in the bootstrap method. For a specific *n* the corresponding point represents the difference between the width associated with *n* measurements and with *n-1* measurements.

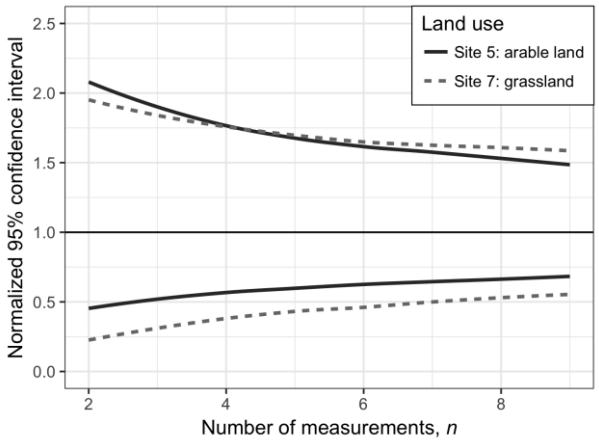

Figure 10 – Normalized 95% confidence intervals by the K_s geometric mean, obtained via the non-parametric bootstrap method for a grassy and an arable plot. The x-axis represents the number of measurements used for each plot.

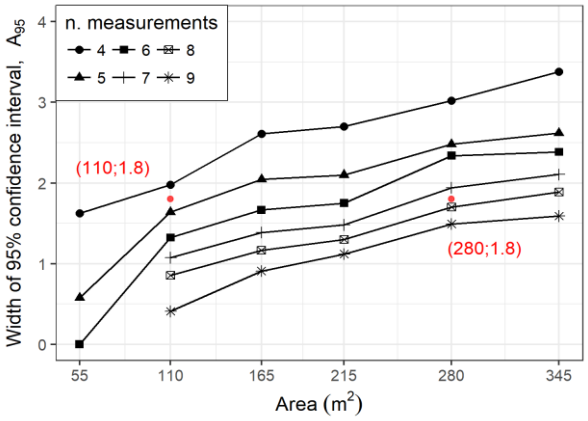

Figure 11 – Width of the 95% confidence intervals normalized by the saturated hydraulic conductivity, K_s, geometric mean plotted against plot size. Lines represent the number of measurements used for the evaluation of the confidence interval and the geometric mean.

Saturated hydraulic conductivity (K_s) greatly influences infiltration modeling

Spatial analysis is performed to understand the controls in agricultural setting

Minimum number of measurements for plot-scale K_s estimate is suggested